Published in Optica 4, issue 12, 1482-1487, 2017
which should be used for any reference to this work

Carrier-envelope offset frequency stabilization of a gigahertz semiconductor disk laser

Nayara Jornod,[1,*] Kutan Gürel,[1] Valentin J. Wittwer,[1] Pierre Brochard,[1] Sargis Hakobyan,[1] Stéphane Schilt,[1] Dominik Waldburger,[2] Ursula Keller,[2] and Thomas Südmeyer[1]

[1]Laboratoire Temps-Fréquence, Université de Neuchâtel, Av. de Bellevaux 51, CH-2000 Neuchâtel, Switzerland
[2]Department of Physics, Institute for Quantum Electronics, ETH Zürich, CH-8093 Zürich, Switzerland
*Corresponding author: nayara.jornod@unine.ch

Optical frequency combs based on ultrafast lasers have enabled numerous scientific breakthroughs. However, their use for commercial applications is limited by the complexity and cost of femtosecond laser technology. Ultrafast semiconductor lasers might change this issue as they can be mass produced in a cost-efficient way while providing large spectral coverage from a single technology. However, it has not been proven to date if ultrafast semiconductor lasers are suitable for stabilization of their carrier-envelope offset (CEO) frequency. Here we present what we believe to be the first CEO frequency stabilization of an ultrafast semiconductor disk laser (SDL). The optically pumped SDL is passively modelocked by a semiconductor saturable absorber mirror. It operates at a repetition rate of 1.8 GHz and a center wavelength of 1034 nm. The 273 fs pulses of the oscillator are amplified to an average power level of 6 W and temporally compressed down to 120 fs. A coherent octave-spanning supercontinuum spectrum is generated in a photonic crystal fiber. The CEO frequency is detected in a standard f–to–$2f$ interferometer and phase locked to an external reference by feedback applied to the current of the SDL pump diode. This proof-of-principle demonstrates that ultrafast SDLs are suitable for CEO stabilization and constitutes a key step for further developments of this comb technology expected in the coming years.

OCIS codes: (140.7260) Vertical cavity surface emitting lasers; (140.5960) Semiconductor lasers; (140.3425) Laser stabilization; (120.3940) Metrology; (140.4050) Mode-locked lasers; (320.6629) Supercontinuum generation.

1. INTRODUCTION

Self-referenced optical frequency combs [1–3] have been revolutionizing numerous areas in metrology and spectroscopy. Today, most comb systems rely on ultrafast Ti:sapphire [4] or fiber lasers [5]. Recently, ultrafast diode-pumped solid-state lasers have also been extensively studied [6], and even diode-pumped Ti:sapphire systems have been presented [7]. However, these technologies are usually complex, bulky, and typically restricted to a narrow wavelength emission band enforced by the gain material. In contrast, semiconductor laser technology offers a simple laser system with the potential of a compact and cheaper solution owing to mass production on the wafer scale. Another key advantage of this technology is the wavelength flexibility inherent to the bandgap engineering, which enables emission at central wavelengths ranging from the ultraviolet to the mid-infrared [8,9]. Moreover, they can easily operate in the gigahertz (GHz) repetition rate regime, which leads to an increased optical power per comb mode and to easier access to individual comb lines. Such performance is attractive for application areas such as the calibration of astronomical spectrographs [10,11], the generation of ultra-low-noise microwave signals [12,13], or molecular spectroscopy [14,15]. Among all ultrafast semiconductor lasers, the semiconductor disk laser (SDL) technology, also called optically pumped vertical external-cavity surface-emitting lasers (VECSELs) [16] has so far achieved the highest average output powers and shortest pulse durations [17,18]. With a semiconductor saturable absorber mirror (SESAM) [19], they provide a simple and compact modelocked laser with the potential for multi-GHz operation [20,21]. For further integration, the SESAM can be combined in the same semiconductor structure as the gain medium, which is referred to as the modelocked integrated external-cavity surface emitting laser (MIXSEL) [22]. VECSELs have been identified as a promising candidate for fully stabilized frequency combs, as they demonstrate low timing jitter and amplitude noise when stabilized in repetition frequency [23]. However, no stabilization of the carrier-envelope offset (CEO) frequency of a VECSEL has been demonstrated so far. The first detection of the CEO beat from a VECSEL was reported in 2014 [24], and required external amplification and compression of the emitted pulses. The insufficient signal-to-noise ratio (SNR) of the CEO beat hindered detailed noise characterization or frequency stabilization of this system. In 2016, we used an indirect

method based on an appropriate combination of different signals from a VECSEL and a continuous-wave laser to characterize both the frequency noise and the modulation bandwidth of the CEO beat for direct pump current modulation [25], without detecting the CEO beat by a standard nonlinear interferometry method [1]. Here we present the first self-referenced stabilization of the CEO frequency of a modelocked semiconductor disk laser with a repetition frequency (f_{rep}) of 1.8 GHz. CEO frequency detection was realized using the standard f–to–$2f$ interferometry technique after amplification and compression of the laser pulses, resulting in a CEO beat note with an SNR of around 30 dB [in a resolution bandwidth (RBW) of 300 kHz]. The stabilization was achieved by direct pump current modulation, resulting in a residual integrated phase noise of 4.5 rad [1 Hz–10 MHz] limited by the amplitude noise of the pump diode. The small footprint of the VECSEL and fiber amplifier enables simple and compact systems that are highly attractive for frequency comb applications. Moreover, the fiber amplifier could be replaced by a few-millimeters-long waveguide amplifier to further simplify and integrate the system [26]. In the near future, we expect that VECSEL-based combs will be able to operate without additional amplifiers, combining the higher peak powers [18,27] with the direct octave-spanning supercontinuum generation (SCG) in silicon nitride waveguides [28].

2. EXPERIMENT AND RESULTS

A. SESAM Modelocked VECSEL

The ultrafast semiconductor disk laser is a VECSEL prototype designed at ETH Zürich. The VECSEL and SESAM structures are described in Ref. [18]. The simple laser cavity consists of only three elements mounted in a V-shaped configuration: the VECSEL gain chip, a SESAM for modelocking operation, and an output coupler with a radius of curvature of 100 mm and a transmission of 1.0%. The cavity length is shorter than 10 cm with a corresponding repetition frequency of 1.8 GHz. The setup is enclosed in an aluminum housing to reduce the influence of external perturbations, such as air flows, leading to a higher stability and lower noise operation of the VECSEL. The temperatures of the SESAM and of the VECSEL chip are regulated to 21°C and 19°C, respectively, by means of thermoelectrical coolers, for more stable operation. The VECSEL gain chip is optically pumped with a typical power of 9 W by a multimode (NA = 0.22, core diameter = 100 μm, $M^2 = 43$) fiber-coupled 808 nm laser diode (LIMO35-F100-DL808-EX2009) that is wavelength stabilized by a volume Bragg grating (VBG). The pump laser is driven in parallel by a high DC current source (Delta Elektronika SM 7.5-80) and a home-built voltage-to-current converter, providing a high bandwidth modulation channel of the pump power for CEO frequency stabilization. We previously measured a modulation bandwidth in the range of 300 kHz (cutoff at −3 dB amplitude or −90° phase shift) for the CEO frequency modulated by the pump power in a similar laser using an indirect method [25]. In addition, a low-pass electrical filter is implemented between the DC current source and the pump diode to filter out the driver noise and to furthermore avoid any cross-talk between the two current drivers.

The laser emits 273 fs pulses at a center wavelength of 1033.9 nm with a spectral full width at half-maximum (FWHM) of 4.6 nm, close to the transform limit (see Fig. 1). The average

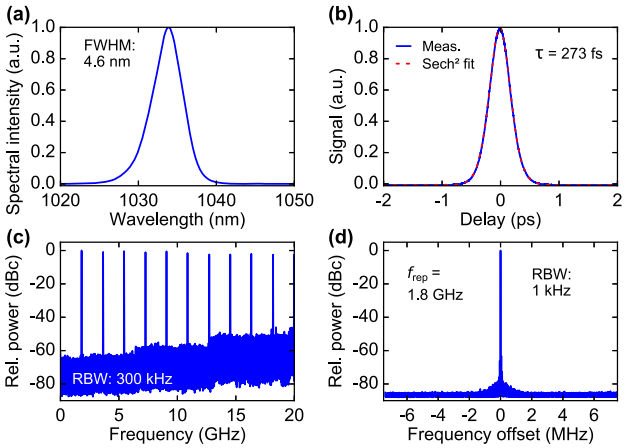

Fig. 1. Characterization of the modelocked VECSEL. (a) Normalized optical spectrum centered at 1033.9 nm with a FWHM of 4.6 nm. (b) Measured autocorrelation trace (blue curve) with corresponding sech^2 fit (dashed red). (c) Microwave spectrum at a RBW of 300 kHz. (d) Microwave spectrum centered at the repetition frequency of 1.8 GHz with a RBW of 1 kHz.

output power is 60 mW, corresponding to a peak power in the range of 100 W. Since this peak power is insufficient for the generation of a coherent supercontinuum (SC) spectrum in a nonlinear fiber, a Yb-fiber amplification stage has been implemented before the self-referencing CEO frequency detection scheme.

An overview of the complete setup is depicted in Fig. 2. An optical isolator is placed at the output of the laser to avoid any backreflection from disturbing the laser operation.

B. Yb-Fiber Amplifier

The amplification stage is made of a 3.5-m-long Yb-doped polarization-maintaining (PM) double-clad fiber with a core diameter of 6 μm (Coractive DF-YB-6/128S-PM). The fiber is pumped in the forward direction by a commercial VBG-stabilized laser diode (Dilas I5F1P15-976.1-25C-HS1.4) emitting at 976 nm (see setup in Fig. 2). A multimode pump combiner (MPC) is spliced to combine the 976 nm pump and the 1034 nm polarized signal. An additional length of ∼40 cm of passive PM fiber is spliced at the end of the gain fiber, where the unabsorbed pump light is removed from the fiber cladding using high refractive index acrylate coating to prevent thermal issues at the fiber tip and the use of an additional optical filter at the output.

The VECSEL seed signal is first sent through polarization selective elements and coupled into a PM fiber with an efficiency of 88%, resulting in a coupled optical power of 46 mW.

The characteristics of the amplifier are shown in Fig. 3. The pump diode delivers output power up to 25 W, from which only 14 W was used for typical operation of the amplifier, generating an amplified signal power of more than 6 W. The corresponding amplification factor is of the order of ∼130 (21 dB), and the extraction efficiency, computed as the ratio between the amplified output power minus the seed power and the pump power, is 44%.

The small core diameter of the gain fiber (6 μm) and the additional passive PM fiber segment enable spectral broadening directly in the amplifier. The 4.6 nm bandwidth (FWHM) of the

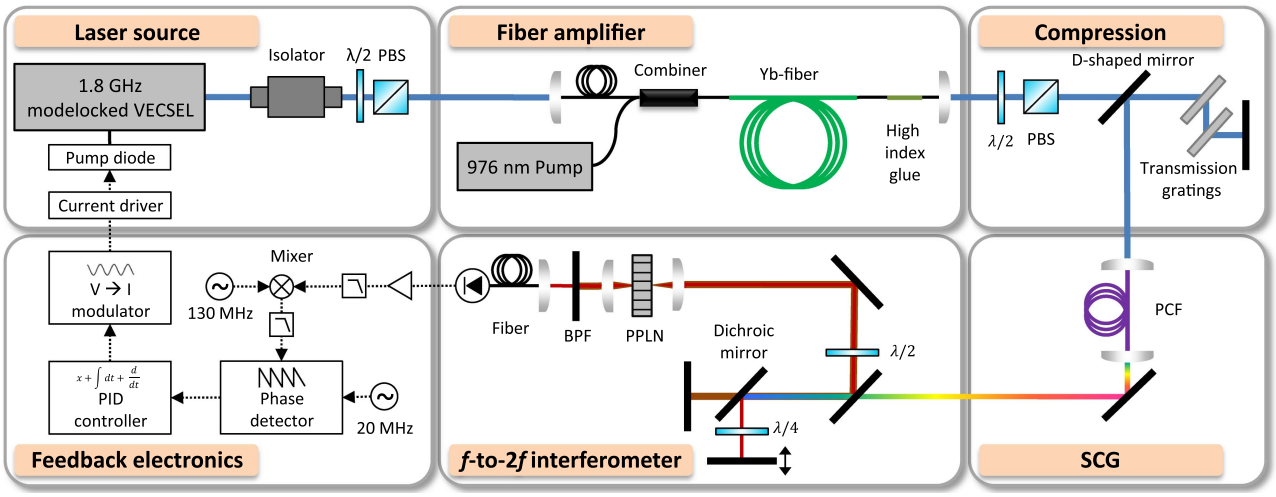

Fig. 2. Diagram of the complete experimental setup made of the ultrafast laser source with its pump diode and current driver, the fiber amplifier, the compression and supercontinuum generation (SCG) stages, the f–to–$2f$ interferometer, and the stabilization electronics. PBS, polarizing beam splitter; PPLN, periodically poled lithium niobate crystal; BPF, bandpass optical filter; PID, proportional-integral-derivative controller.

laser optical spectrum is broadened to more than 25 nm in the amplifier [Fig. 3(a)]. During amplification, the temporal pulse duration is also broadened to more than 2 ps.

The amplified pulses are then temporally compressed in two transmission gratings in a double-pass configuration (Fig. 2). At the output, the pulse duration is reduced to sub-120-fs with an average power at the 3 W level. The autocorrelation trace of the compressed pulses [Fig. 3(b)] shows small distortions from a sech^2 pulse shape. We believe that a nonlinear chirp is induced during the amplification process, which prevents the compression from achieving the transform-limited pulse duration supported by the optical bandwidth.

The phase noise of the repetition frequency of the optical pulses measured before and after amplification shows a negligible contribution of the amplifier [Fig. 3(e)]; only significant additional amplitude modulation (AM) noise at frequencies below 100 Hz is observed, increasing the root mean square (RMS) AM noise from 0.2% to 0.9% (1 Hz–30 MHz) [Fig. 3(d)].

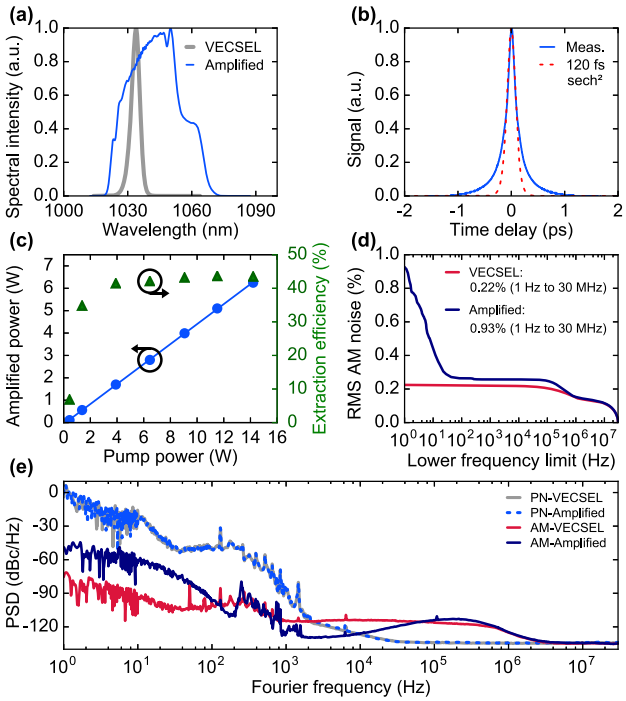

Fig. 3. Characterization of the fiber amplifier. (a) Normalized optical spectrum of the signal after amplification. (b) Autocorrelation trace of the compressed pulses (blue) and comparison with a 120 fs sech^2 pulse. (c) Amplified signal power as a function of the pump power (blue, left axis) and corresponding extraction efficiency (green, right axis). (d) RMS AM noise as a function of the lower frequency integration limit. (e) Phase noise (PN) power spectral density (PSD) of the repetition frequency before (gray) and after (dashed light blue) the amplification, and AM noise of the repetition frequency before (red) and after (dark blue) the amplification.

C. CEO Beat Detection

After compression, an average power of 1.65 W is finally coupled into an angle-polished, collapsed 1-m-long photonic crystal fiber (PCF, NKT Photonics NL-3.2-945), corresponding to a coupling efficiency of ~80%, to generate a coherent octave-spanning SC spectrum [see Fig. 4(a)].

The SC light is sent to a quasi-common path f–to–$2f$ interferometer schematized in the bottom part of Fig. 2. The 700 nm and 1400 nm components of the spectrum are separated by a dichroic mirror. An adjustable delay line in the low wavelength path enables its temporal tuning. The two spectral components

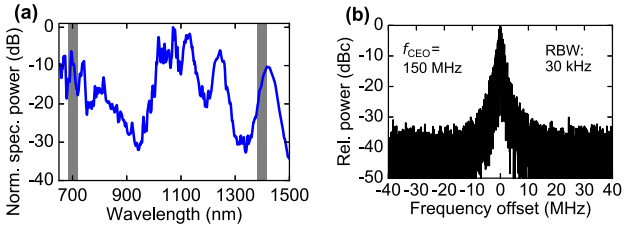

Fig. 4. (a) Measured octave-spanning SC spectrum generated in the PCF. The gray spectral bands centered at 700 nm and 1400 nm are used for CEO beat detection in the f–to–$2f$ interferometer. (b) Detected free-running CEO beat at 150 MHz with a RBW of 30 kHz.

are then recombined using the same mirror and co-propagate through a magnesium-oxide-doped periodically poled lithium niobate (MgO:PPLN) crystal where the 1400 nm light is frequency-doubled (poling period 14 μm, crystal temperature 70°C). A half-wave plate is placed in the common path before the crystal for optimization of the second harmonic generation (SHG) process, and a quarter-wave plate is used in the 700 nm adjustable delay line to align the polarization of the two beams.

The resulting 700 nm light from the two beams is optically bandpass filtered at the output of the crystal and is coupled into a single-mode fiber to ensure an optimum spatial overlap. Their beat signal is detected using a variable-gain avalanche photodetector (Thorlabs APD430A/M) with a bandwidth of 400 MHz for stabilization and a fast photodetector (New Focus 1014, 45 GHz bandwidth) for static tuning curve measurements. The detected CEO beat has an SNR of ∼30 dB in a 300 kHz RBW. Figure 4(b) shows the typical free-running CEO beat measured at ∼150 MHz and used later for stabilization. The photodiode output signal is bandpass filtered and amplified. We observed a strong dependence of the CEO frequency f_{CEO} to the operation mode of the VECSEL. Changes in the laser parameters (such as fine cavity alignment, pump power, gain, or SESAM temperature) were used to efficiently tune the CEO beat note to a desired frequency in the detector bandwidth. A characterization of the tuning curve of f_{CEO} as a function of the current of the VECSEL pump diode is shown in Fig. 5(a) for CEO frequencies in the range of 500 MHz. The tuning coefficient is ∼0.3 MHz/mA.

The dynamic response of f_{CEO} to a modulation of the pump current was measured in amplitude and phase using a frequency discriminator [29] and a lock-in amplifier (Zurich Instrument HF2LI). The measured transfer function has a −3 dB cutoff frequency of ∼300 kHz with a corresponding phase shift of approximately −90° [see Fig. 5(b)]. This result is in good agreement with our previous measurement performed indirectly in a similar laser without detecting the CEO beat by f–to–$2f$ interferometry [25]. In addition, we also measured the transfer function of the optical power of the pump diode [see orange curves in Fig. 5(b)]. The observed modulation bandwidth is larger than 1 MHz, which is broader than the measured response of f_{CEO}. Therefore, the modulation bandwidth of f_{CEO} is neither limited by the pump driving electronics, nor by the modulation response of the pump diode itself, but more likely by the cavity dynamics in our laser (the short upper-state lifetime in the semiconductor gain is not expected to be a limitation).

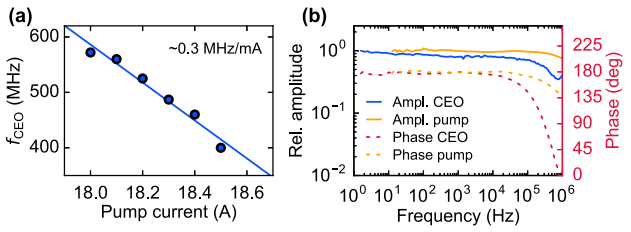

Fig. 5. (a) Static tuning curve of the CEO frequency with the pump current. (b) Left axis: relative amplitude of the transfer functions of the pump optical power (orange) and of f_{CEO} (blue) for a modulation of the pump current. Right axis: phase of the transfer functions of the pump optical power (dashed orange) and of f_{CEO} (red) for a modulation of the pump current.

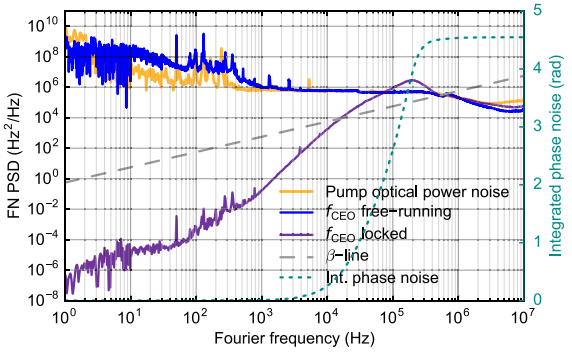

Fig. 6. Left axis: measured frequency noise PSD of the free-running (blue) and stabilized (violet) CEO signal, and pump-induced frequency noise (orange) calculated from the measured pump RIN multiplied by the pump-power-to-f_{CEO} transfer function. Right axis: integrated phase noise of the stabilized CEO signal as a function of the upper cut-off frequency.

We measured the frequency noise power spectral density (FN–PSD) of the free-running CEO beat using a phase noise analyzer (Rohde–Schwarz FSWP26). The result is presented in Fig. 6 (blue curve). The corresponding free-running CEO linewidth calculated using the approximation of the β–separation line [30] is 1.3 MHz (at 1 s integration time). A feedback bandwidth in the range of 600 kHz is estimated to be necessary to achieve a tight CEO lock from the crossing point of the CEO FN-PSD with the β–separation line. This is 2 times larger than our previous estimation made for a similar VECSEL without directly detecting the CEO beat [25]. The reason is the higher frequency noise observed here at Fourier frequencies above ∼1 kHz compared to the $1/f$ noise behavior extrapolated in our previous study, where the noise measurement was limited by the experimental noise floor at high Fourier frequencies. To understand the origin of this high frequency noise plateau observed at Fourier frequencies between 1 kHz and ∼300 kHz, we investigated the contribution of the pump noise. We measured the relative intensity noise (RIN) of the pump diode and calculated its contribution to the CEO FN-PSD using the previously recorded frequency response of f_{CEO} for pump current modulation (Fig. 5). The resulting pump-induced frequency noise, depicted in orange in Fig. 6, overlaps fairly well with the measured free-running CEO FN-PSD at Fourier frequencies above 1 kHz, demonstrating that the high f_{CEO} noise originates from the AM noise of the pump diode.

D. CEO Stabilization

The amplified CEO beat note was first frequency down-converted to ∼20 MHz for comparison to a reference signal from a function generator in a digital phase detector (Menlo Systems DXD200; see bottom part of Fig. 2). The phase error signal was sent to an analog proportional-integral-derivative (PID) servo-controller (Vescent Photonics D2–125) and the feedback signal was directly applied to our home-built voltage-to-current converter to modulate the VECSEL pump power. The FN-PSD of the stabilized CEO beat displayed in violet in Fig. 6 shows a clear noise reduction compared to the free-running CEO beat signal at Fourier frequencies up to ∼100 kHz. The FN-PSD is reduced below the β–separation line at all frequencies below

~20 kHz, but it remains above the line in the range of 20–500 kHz, especially at the servo bump (~200 kHz). As a consequence, a tight CEO lock is not achieved in the present situation, and the integrated phase noise is 4.5 rad [1 Hz–10 MHz]. As shown in Section 2.C, the AM noise of the pump diode is responsible for the free-running f_{CEO} noise at frequencies above 1 kHz, increasing the necessary feedback bandwidth and preventing the achievement of a tight lock.

The achieved integrated phase noise does not compete with the performance reached today by established femtosecond frequency combs, such as 14 mrad integrated phase noise demonstrated by a monolithic Er:Yb:glass laser ($f_{rep} = 1$ GHz) [31], 29 mrad from a Ti:sapphire laser ($f_{rep} = 75$ MHz) [32], or 68 mrad (out-of-loop) from an Er:fiber laser ($f_{rep} = 250$ MHz) with the use of a high bandwidth intra-cavity actuator [33]. However, this is a similar situation than for the first proof-of-principle demonstrations of other comb technologies, such as the first Er:fiber comb that operated at 50 MHz repetition rate with ~20 rad integrated phase noise (computed by upscaling the measured 50 mrad phase noise of the frequency-divided CEO beat by the division factor of 400) [34].

3. CONCLUSION

We have demonstrated what is, to the best of our knowledge, the first CEO frequency stabilization of a modelocked semiconductor laser. The 1.8 GHz VECSEL is amplified and spectrally broadened in a double-clad fiber amplifier, enabling 120 fs pulses and the generation of a coherent octave-spanning SC spectrum. The CEO frequency is detected with an f–to–$2f$ interferometer at an SNR of ~30 dB (300 kHz RBW), which is sufficient for stabilization. Although the VECSEL is pumped by a highly multimode ($M^2 = 43$) fiber-coupled diode laser, we were able to stabilize the CEO beat note via modulation of the pump laser current with a residual integrated phase noise of 4.5 rad [1 Hz–10 MHz].

The high frequency noise of the CEO beat that prevents the achievement of a better lock was shown to originate from the AM noise of the pump diode. Therefore, reducing this noise would lower the CEO noise. This could be achieved by investigating the use of other pump sources or by implementing an amplitude stabilization of the pump that might significantly reduce the noise level. Combining two feedback loops to the pump current acting in different bandwidths on the pump power and CEO frequency could be a way to reduce the CEO phase noise and improve the lock performance.

Finally, another alternative to increase the bandwidth of the CEO corrections and reduce the residual CEO noise would be to implement a feedforward loop using a frequency shifter acousto-optic modulator, as previously demonstrated with a Ti:sapphire comb [35] instead of the feedback loop used here.

Moreover, the ultrafast VECSEL technology is steadily evolving, and recently 101 fs pulses with 1 kW peak power were demonstrated [36]. This peak power level and pulse duration appear sufficient to suppress the amplification stage and generate the octave-spanning SC directly in millimeter-long silicon nitride waveguides [28].

Funding. Nano-Tera.ch MIXSEL II (20NA21_145932).

REFERENCES

1. H. R. Telle, G. Steinmeyer, A. E. Dunlop, J. Stenger, D. H. Sutter, and U. Keller, "Carrier-envelope offset phase control: a novel concept for absolute optical frequency measurement and ultrashort pulse generation," Appl. Phys. B **69**, 327–332 (1999).
2. D. J. Jones, S. A. Diddams, J. K. Ranka, A. Stentz, R. S. Windeler, J. L. Hall, and S. T. Cundiff, "Carrier-envelope phase control of femtosecond mode-locked lasers and direct optical frequency synthesis," Science **288**, 635–639 (2000).
3. A. Apolonski, A. Poppe, G. Tempea, C. Spielmann, T. Udem, R. Holzwarth, T. W. Hänsch, and F. Krausz, "Controlling the phase evolution of few-cycle light pulses," Phys. Rev. Lett. **85**, 740–743 (2000).
4. A. Bartels, D. Heinecke, and S. A. Diddams, "10-GHz self-referenced optical frequency comb," Science **326**, 681 (2009).
5. M. E. Fermann and I. Hartl, "Ultrafast fiber laser technology," IEEE J. Sel. Top. Quantum Electron. **15**, 191–206 (2009).
6. S. Hakobyan, V. J. Wittwer, P. Brochard, K. Gürel, S. Schilt, A. S. Mayer, U. Keller, and T. Südmeyer, "Full stabilization and characterization of an optical frequency comb from a diode-pumped solid-state laser with GHz repetition rate," Opt. Express **25**, 20437–20453 (2017).
7. K. Gürel, V. J. Wittwer, S. Hakobyan, S. Schilt, and T. Südmeyer, "Carrier envelope offset frequency detection and stabilization of a diode-pumped mode-locked Ti:sapphire laser," Opt. Lett. **42**, 1035–1038 (2017).
8. S.-H. Park, J. Kim, H. Jeon, T. Sakong, S.-N. Lee, S. Chae, Y. Park, C.-H. Jeong, G.-Y. Yeom, and Y.-H. Cho, "Room-temperature GaN vertical-cavity surface-emitting laser operation in an extended cavity scheme," Appl. Phys. Lett. **83**, 2121–2123 (2003).
9. M. Rahim, M. Arnold, F. Felder, K. Behfar, and H. Zogg, "Midinfrared lead-chalcogenide vertical external cavity surface emitting laser with 5 μm wavelength," Appl. Phys. Lett. **91**, 151102 (2007).
10. C.-H. Li, A. J. Benedick, P. Fendel, A. G. Glenday, F. X. Kärtner, D. F. Phillips, D. Sasselov, A. Szentgyorgyi, and R. L. Walsworth, "A laser frequency comb that enables radial velocity measurements with a precision of 1 cm s^{-1}," Nature **452**, 610–612 (2008).
11. T. Steinmetz, T. Wilken, C. Araujo-Hauck, R. Holzwarth, T. W. Hänsch, L. Pasquini, A. Manescau, S. D'Odorico, M. T. Murphy, T. Kentischer, W. Schmidt, and T. Udem, "Laser frequency combs for astronomical observations," Science **321**, 1335–1337 (2008).
12. T. M. Fortier, M. S. Kirchner, F. Quinlan, J. Taylor, J. C. Bergquist, T. Rosenband, N. Lemke, A. Ludlow, Y. Jiang, C. W. Oates, and S. A. Diddams, "Generation of ultrastable microwaves via optical frequency division," Nat. Photonics **5**, 425–429 (2011).
13. X. Xie, R. Bouchand, D. Nicolodi, M. Giunta, W. Hänsel, M. Lezius, A. Joshi, S. Datta, C. Alexandre, M. Lours, P.-A. Tremblin, G. Santarelli, R. Holzwarth, and Y. L. Coq, "Photonic microwave signals with zeptosecond-level absolute timing noise," Nat. Photonics **11**, 44–47 (2017).
14. S. Schiller, "Spectrometry with frequency combs," Opt. Lett. **27**, 766–768 (2002).
15. S. M. Link, D. J. H. C. Maas, D. Waldburger, and U. Keller, "Dual-comb spectroscopy of water vapor with a free-running semiconductor disk laser," Science **356**, 1164–1168 (2017).
16. O. G. Okhotnikov, *Semiconductor Disk Lasers: Physics and Technology* (Wiley, 2010).
17. B. Rudin, V. J. Wittwer, D. J. H. C. Maas, M. Hoffmann, O. D. Sieber, Y. Barbarin, M. Golling, T. Südmeyer, and U. Keller, "High-power MIXSEL: an integrated ultrafast semiconductor laser with 6.4 W average power," Opt. Express **18**, 27582–27588 (2010).
18. D. Waldburger, S. M. Link, M. Mangold, C. G. E. Alfieri, E. Gini, M. Golling, B. W. Tilma, and U. Keller, "High-power 100 fs semiconductor disk lasers," Optica **3**, 844–852 (2016).
19. U. Keller, K. J. Weingarten, F. X. Kärtner, D. Kopf, B. Braun, I. D. Jung, R. Fluck, C. Hönninger, N. Matuschek, and J. Aus der Au, "Semiconductor saturable absorber mirrors (SESAM's) for femtosecond to nanosecond pulse generation in solid-state lasers," IEEE J. Sel. Top. Quantum Electron. **2**, 435–453 (1996).
20. B. W. Tilma, M. Mangold, C. A. Zaugg, S. M. Link, D. Waldburger, A. Klenner, A. S. Mayer, E. Gini, M. Golling, and U. Keller, "Recent advances in ultrafast semiconductor disk lasers," Light Sci. Appl. **4**, e310 (2015).
21. D. Lorenser, D. J. H. C. Maas, H. J. Unold, A.-R. Bellancourt, B. Rudin, E. Gini, D. Ebling, and U. Keller, "50-GHz passively mode-locked

surface-emitting semiconductor laser with 100-mW average output power," IEEE J. Quantum Electron. **42**, 838–847 (2006).
22. D. J. H. C. Maas, A.-R. Bellancourt, B. Rudin, M. Golling, H. J. Unold, T. Südmeyer, and U. Keller, "Vertical integration of ultrafast semiconductor lasers," Appl. Phys. B **88**, 493–497 (2007).
23. V. J. Wittwer, R. van der Linden, B. W. Tilma, B. Resan, K. J. Weingarten, T. Südmeyer, and U. Keller, "Sub-60-fs timing jitter of a SESAM mode-locked VECSEL," IEEE Photon. J. **5**, 1400107 (2013).
24. C. A. Zaugg, A. Klenner, M. Mangold, A. S. Mayer, S. M. Link, F. Emaury, M. Golling, E. Gini, C. J. Saraceno, B. W. Tilma, and U. Keller, "Gigahertz self-referenceable frequency comb from a semiconductor disk laser," Opt. Express **22**, 16445–16455 (2014).
25. P. Brochard, N. Jornod, S. Schilt, V. J. Wittwer, S. Hakobyan, D. Waldburger, S. M. Link, C. G. E. Alfieri, M. Golling, L. Devenoges, J. Morel, U. Keller, and T. Südmeyer, "First investigation of the noise and modulation properties of the carrier-envelope offset in a modelocked semiconductor laser," Opt. Lett. **41**, 3165–3168 (2016).
26. N. Jornod, V. J. Wittwer, C. Kränkel, D. Waldburger, U. Keller, T. Südmeyer, and T. Calmano, "High-power amplification of a femtosecond vertical external-cavity surface-emitting laser in an Yb:YAG waveguide," Opt. Express **25**, 16527–16533 (2017).
27. K. G. Wilcox, A. C. Tropper, H. E. Beere, D. A. Ritchie, B. Kunert, B. Heinen, and W. Stolz, "4.35 kW peak power femtosecond pulse mode-locked VECSEL for supercontinuum generation," Opt. Express **21**, 1599–1605 (2013).
28. A. R. Johnson, A. S. Mayer, A. Klenner, K. Luke, E. S. Lamb, M. R. E. Lamont, C. Joshi, Y. Okawachi, F. W. Wise, M. Lipson, U. Keller, and A. L. Gaeta, "Octave-spanning coherent supercontinuum generation in a silicon nitride waveguide," Opt. Lett. **40**, 5117–5120 (2015).
29. S. Schilt, N. Bucalovic, L. Tombez, V. Dolgovskiy, C. Schori, G. Di Domenico, M. Zaffalon, and P. Thomann, "Frequency discriminators for the characterization of narrow-spectrum heterodyne beat signals: application to the measurement of a sub-Hertz carrier-envelope-offset beat in an optical frequency comb," Rev. Sci. Instrum. **82**, 123116 (2011).
30. G. Di Domenico, S. Schilt, and P. Thomann, "Simple approach to the relation between laser frequency noise and laser line shape," Appl. Opt. **49**, 4801–4807 (2010).
31. T. D. Shoji, W. Xie, K. L. Silverman, A. Feldman, T. Harvey, R. P. Mirin, and T. R. Schibli, "Ultra-low-noise monolithic mode-locked solid-state laser," Optica **3**, 995–998 (2016).
32. T. J. Yu, K.-H. Hong, H.-G. Choi, J. H. Sung, I. W. Choi, D.-K. Ko, J. Lee, J. Kim, D. E. Kim, and C. H. Nam, "Precise and long-term stabilization of the carrier-envelope phase of femtosecond laser pulses using an enhanced direct locking technique," Opt. Express **15**, 8203–8211 (2007).
33. W. Hänsel, M. Giunta, K. Beha, M. Lezius, M. Fischer, and R. Holzwarth, "Ultra-low phase noise all-PM Er:fiber optical frequency comb," in *Advanced Solid State Lasers* (Optical Society of America, 2015), paper ATh4A.2.
34. B. R. Washburn, S. A. Diddams, N. R. Newbury, J. W. Nicholson, M. F. Yan, and C. G. Jørgensen, "Phase-locked, erbium-fiber-laser-based frequency comb in the near infrared," Opt. Lett. **29**, 250–252 (2004).
35. S. Koke, A. Anderson, H. Frei, A. Assion, and G. Steinmeyer, "Noise performance of a feed-forward scheme for carrier-envelope phase stabilization," Appl. Phys. B **104**, 799–804 (2011).
36. D. Waldburger, C. G. E. Alfieri, S. M. Link, E. Gini, M. Golling, and U. Keller, "High-power semiconductor disk lasers with record-short pulse durations," in *European Conference on Lasers and Electro-Optics—European Quantum Electronics Conference* (Optical Society of America, 2017), paper CB-8.1.